DETERMINATION OF THE PROPER MOTION RANGE FOR THE ROTARY ACTUATORS OF 6-RSS PARALLEL ROBOT

Rui Zeng[1], Shuling Dai[1], Wenfang Xie[2], Xiaoming Zhang[3]
[1]*State Key Laboratory of Virtual Reality Technology and Systems, Beihang University,Beijing,R.P.China*
[2]*Department of Mechanical & Industrial Engineering, Concordia University, Montreal, Canada*
Email: zeng.rui.rigg@gmail.com;wfxie@encs.concordia.ca

ABSTRACT

The 6-DOFs parallel robots with RSS structure have a unique kinematic characteristic as their actuators are limited in circular orbits. In this paper, the kinematic knowledge is used to obtain the proper motion range for the actuators of this kind of parallel robots. The available workspace analysis is presented firstly to obtain the minimum range of actuators. Then the simple singularity constraint for RSS structure parallel robot is given to certify the singularity-free motion range of actuators. A novel direct kinematic algorithm based on the mechanism deformation is introduced latter for unique direct kinematic solutions' determination during motion range optimization procedure. Simulation results demonstrate that the proposed methods can provide a proper motion range, in which the end-effector covers the biggest reachable workspace with a singularity-free, unique determined actuators' motion.

Keywords: parallel robot; workspace; singularity; direct kinematic.

DÉTERMINATION DE LA MOTION GAMME APPROPRIÉE POUR LES ACTIONNEURS ROTARY DE ROBOT PARALLÈLE 6-RSS

RÉSUMÉ

Les robots parallèles à 6 degrés de liberté avec la structure RSS ont une caractéristique cinématique unique que leurs actionneurs sont limitées dans des orbites circulaires. Dans cet article, les connaissances cinématiques sont utilisées pour obtenir la gamme de mouvement propre pour les actionneurs. L'analyse de l'espace de travail disponible est présentée en premier lieu, qui peut être utilisé pour déterminer la distance minimale d'actionneurs. Puis la contrainte de la singularité spéciale pour la structure RSS robot parallèle est donnée pour certifier le non-singularité de lieu géométrique d'actionneurs. Ensuite, un nouvel algorithme cinématique directe fondée sur la déformation du mécanisme est introduit pour trouver la condition unique des solutions cinématiques. Enfin, nous obtenons la gamme de propre mouvement, dans laquelle l'effecteur couvre l'ensemble espace de travail accessible avec la motion d'actionneurs sans singularité, uniquement déterminés.

Mots-clés : robot parallèle ; espace de travail ; singularité ; cinématique directe.

1. INTRODUCTION

Various parallel robots with six degree of freedom have been widely used in many fields including flight simulators, parallel robot manipulators, machining tools and 6-DOF coordinate measuring devices [1]. Compared to other kinds of parallel robot, the 6-DOF RSS structure parallel robots (or 6-RSS parallel robots) have special kinematic characteristics because of their limited actuator orbits. As we usually assume that the number of limbs for the parallel robot is equal to its degree of freedom, and only one actuator is needed for each limb [2], then based on the Chebychev–Grübler–Kutzbach criterion [3], each limb of the 6-DOF parallel robots should be a 6-DOF serial chain. Once one revolute joint and two spherical joints are applied in one limb, the only chain structure for 6-DOF is R-S-S(in which the two adjacent spherical joints can remove the redundant freedom). Hence, from kinematic point of view, the 6-RSS structure parallel robots is equivalent to the 6-RUS or 6-RSU structure robots. Since the first time conducted by Hunt [4], the kinematic research on 6-RSS parallel robot has attracted a great attention and normally covers workspace representation, singularity analysis and direct kinematic solution determination.

The workspace of 6-DOF parallel robot is hard to compute and express [5], because it is a complex six dimensional volume with non-linear boundaries. To visualize the workspace, both constant-orientation workspace in the Cartesian space [6] and constant-position workspace [7] in the Orientation space.

The singularity of 6-DOF parallel robot is the special mechanism status where the resultant torque from actuators acted upon the end-effector degenerates into a dimension less than six. There are various of singularity analysis methods for 6-DOF parallel robot that have been applied by researchers, such as the line geometric method [8], screw theory method [9], differential geometric method [10, 11], torque analysis [12] and pure geometric method [13]. The common feature of these methods is that they concentrate on the efficient utilization of Jacobian matrix. The Jacobian matrix of 6-RSS parallel robot indicates both the mechanical singularities (singularity-II in [13]or over-mobility in [14]), and the serial singularities (singularity-I in [13]or under-mobility in [14]). Isidro Zabalza redefined the serial singularities of 6-RSS parallel robot as “stationary configurations” (SCs) and determined the actuators perturbations insensitive configurations based on 64 special SCs [15]. The serial singularities are usually known as "limit points" in the mechanism system (especially serial robot system) with rotary actuator, and we use the word "bifurcation" instead here to reveal its relationship with direct kinematic solutions.

Direct kinematic, or forward kinematic, is referred to as the calculation of the end-effector’s position from given values of special joints(especially actuator joints). For the most 6-DOF parallel robot, the nonlinear direct kinematic equations can be solved by the algorithms like Newton method [16], homotopy method [17], neural network [18, 19], algebraic elimination [20]. The singularities usually drive the direct kinematic algorithm of 6-DOF parallel robot to converge into wrong solutions if improper initial value is chosen. Especially for the 6-RSS parallel robot, the solution to direct kinematic is easy to be trapped by the local minimum due to both the mechanical singularities and serial singularities.

For a given 6-DOF parallel robot, the kinematic analysis usually leads to the constraint conditions determination for proper end-effector motion domain or pose. Jiang utilized the orientation fixed singularity surface of a 6-DOF Stewart-Gough platform as the constrain conditions of maximal singularity-free workspace optimization [21]. Li obtained similar singularity-free workspace of a 6-RSS parallel robot by using a boundary searching algorithm based on the determinant of Jacobian matrix [22]. Martinez found the proper initial pose for the algorithm which results in a fast convergence into the right kinematic solution [23], while most robust direct kinematic algorithms are trying to find a proper domain in which the desired direct kinematic solution is unique and easy to obtain. Similarly, this paper aims to obtain the common kinematic constraint conditions of 6-RSS parallel robot for a proper motion domain determination. Compared to the complex six-dimensional workspace, a proper motion range for the actuators is more convenient for application purpose. Coste defined the singularity-free workspace of a 3RPR manipulator by the length

range of actuator legs [24]. Zeng determined a proper motion range of legs for the Stewart-Gough platform with both singularity-free and homeomorism constraint conditions [25]. In this research, we try to obtain the proper actuators motion range for the parallel robot with the kinematic constraint principles such as: exploiting the best potential of the actuators, finding the singularity-free and the unique direct solution in the whole motion range.

This paper is organized as follows. Some basic knowledge of the 6-RSS parallel robot and details for the actuator motion range are introduced in Section 2. The main methods for the proper actuator motion range determination are presented in Section 3. In Section 4, the proper actuator motion range for a six-rotary-axis-parallel 6-RSS robot is optimized. And finally, the conclusion is drawn and some potential future work is given in Section 5.

2. THE BASIC KNOWLEDGE FOR 6-RSS PARALLEL ROBOT

2.1. Kinematic modeling and definition

For the parallel robots with m rotary actuators (the outputs denoted by $\theta_i (i = 1,2,...,m)$), if the end-effector posture is denoted as $\mathbf{p}$, the kinematic can be represented by the constant distance l_i between the end-effector terminals $A_i(\mathbf{p})$ and the rotation determined terminals $T_i(\theta_i)$. The common algebraic formula for these parallel robots is given as follows:

$$l_i = \|A_i(\mathbf{p}) - T_i(\theta_i)\|_2 \, (i = 1,2,...,m). \tag{1}$$

When more details in the chain are considered, as shown in Fig.1, Eq. (1) can be rewritten as follows:

$$l_{A_iT_i} = \|A_i(\mathbf{p}) - T_i(\theta_i, l_{T_iB_i}, w_i, B_i)\|_2 \, (i = 1,2,...,6) \tag{2}$$

where $l_{A_iT_i}$ is the distance between A_i and T_i, $l_{T_iB_i}$ is the distance between T_i and B_i, w_i is the actuator rotary axis unit vector for the i^{th} chain, B_i is the base terminal for the i^{th} chain. And shown as Fig.2, in each chain which links the end-effector and the base, the following relationship exists

$$OO' = OB_i + B_iT_i + T_iA_i + A_iO' (i = 1,2,...,6). \tag{3}$$

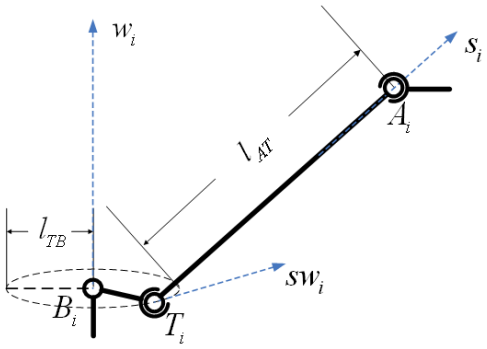

Fig. 1. Single RSS chain in parallel robot

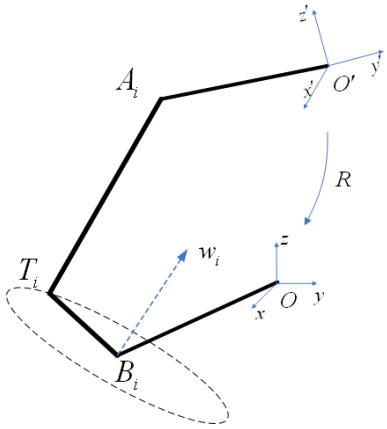

Fig. 2. Single closed-loop in parallel robot

We denote $x'y'z'o'$ as the end-effector coordinate frame with origin O', $xyzo$ as the world coordinate frame with origin O, then the three main differences between various types of 6-RSS parallel robots can be concluded as: the position of A_i in $x'y'z'o'$ frame; the position of B_i in $xyzo$ frame; and the value of w_i in $xyzo$ frame. In Hunt robot, six rotary axes share a plane when the end-effector terminals coincide at three points [4]. The Hexa manipulator, which expanded from Hunt robot, owns a hexagonal end-effector with six A_i terminals [14]. A 6-RSS parallel robot introduced in [12] shares one base terminal and common rotary axis. Eq. (3) is a concise version of the kinematic model for RSS structural parallel robot. As shown in

the following Eqs. (4) and (5), we can build the kinematic mapping between the end-effector position and actuators' rotation angles by determining all the terminal points' coordinates if $w_i = [x_{wi}, y_{wi}, z_{wi}]^T$.

$$\begin{cases} (x_{ti}-x_{ai})^2+(y_{ti}-y_{ai})^2+(z_{ti}-z_{ai})^2 = & l_{A_iT_i}^2 \\ (x_{ti}-x_{bi})^2+(y_{ti}-y_{bi})^2+(z_{ti}-z_{bi})^2 = & l_{T_iB_i}^2 \\ (x_{ti}-x_{bi})\,x_{wi}+(y_{ti}-y_{ai})\,y_{wi}+(z_{ti}-z_{ai})\,z_{wi} = & 0 \end{cases} \tag{4}$$

$$\begin{bmatrix} x_{ti} \\ y_{ti} \\ z_{ti} \end{bmatrix} = \begin{bmatrix} \cos(\theta_i+\theta_{0,i}) & -\sin(\theta_i+\theta_{0,i}) & 0 \\ \sin(\theta_i+\theta_{0,i}) & \cos(\theta_i+\theta_{0,i}) & 0 \\ 0 & 0 & 1 \end{bmatrix} \begin{bmatrix} \frac{y_{wi}}{\sqrt{x_{wi}^2+y_{wi}^2}} & \frac{x_{wi}}{\sqrt{x_{wi}^2+y_{wi}^2}} & 0 \\ \frac{-x_{wi}z_{wi}}{\sqrt{x_{wi}^2+y_{wi}^2}} & \frac{y_{wi}z_{wi}}{\sqrt{x_{wi}^2+y_{wi}^2}} & \sqrt{1-z_{wi}^2} \\ \frac{x_{wi}\sqrt{1-z_{wi}^2}}{\sqrt{x_{wi}^2+y_{wi}^2}} & \frac{-y_{wi}\sqrt{1-z_{wi}^2}}{\sqrt{x_{wi}^2+y_{wi}^2}} & z_{wi} \end{bmatrix} \begin{bmatrix} l_{T_iB_i} \\ 0 \\ 0 \end{bmatrix} \tag{5}$$

where $[x_{ai}, y_{ai}, z_{ai}]^T$, $[x_{bi}, y_{bi}, z_{bi}]^T$ and $[x_{ti}, y_{ti}, z_{ti}]^T$ are the coordinate value for A_i, B_i and T_i in $xyzo$ frame respectively, $\theta_{0,i}$ is the initial actuator angle in the i^{th} chain compared to the positive direction of x axis and θ_i is the rotary actuator output angle in the i^{th} chain corresponding $\theta_{0,i}$.

2.2. Inverse Kinematic of the parallel robot

The inverse kinematic of 6-RSS parallel robot can deduce the rotation angles of actuators from the known end-effector position with the constraints of Eqs. (4) and (5). Solved from Eq. (4), the common inverse kinematic solution for 6-RSS structural parallel robot is given as follows:

$$\begin{cases} x_{ti} = & \dfrac{m_{4i}y_{wi}+(n_{2i}z_{wi}-n_{3i}y_{wi})(z_{ti}-z_{bi})}{n_{1i}y_{wi}-n_{2i}x_{wi}}+x_{bi} \\ y_{ti} = & \dfrac{m_{4i}x_{wi}+(n_{1i}z_{wi}-n_{3i}x_{wi})(z_{ti}-z_{bi})}{n_{2i}x_{wi}-n_{1i}y_{wi}}+y_{bi} \\ z_{ti} = & \dfrac{-m_{2i}\pm\sqrt{m_{2i}^2-4m_{1i}m_{3i}}}{2m_{1i}}+z_{bi} \end{cases} \tag{6}$$

where $n_{1i}=x_{bi}-x_{ai}, n_{2i}=y_{bi}-y_{ai}, n_{3i}=z_{bi}-z_{ai}, m_{1i}=(n_{2i}z_{wi}-n_{3i}y_{wi})^2+(n_{1i}z_{wi}-n_{3i}x_{wi})^2+(n_{1i}y_{wi}-n_{2i}x_{wi})^2$, $m_{2i}=2y_{wi}m_{4i}(n_{2i}z_{wi}-n_{3i}y_{wi})+2x_{wi}m_{4i}(n_{1i}z_{wi}-n_{3i}x_{wi})$, $m_{3i}=y_{wi}^2m_{4i}^2+x_{wi}^2m_{4i}^2-l_{TB}^2$, $m_{4i}=l_{TB}^2-l_{AT}^2+n_{1i}^2+n_{2i}^2+n_{3i}^2$.

Similar works have been done in [12, 14, 26], but the inverse kinematic solutions in those papers are just given for one special kind of 6-RSS parallel robot. The special inverse kinematic solution for the 6-RSS parallel robot that will be introduced in Section 4 is shown in Eqs. (7) and (8), in which rotary axis vector $w_i=[0,0,1]^T$ and $z_{ti}=z_{bi}$.

$$\begin{cases} x_{ti} = & -\dfrac{y_{ai}-y_{bi}}{x_{ai}-x_{bi}}y_{ti}+\dfrac{N_{1i}}{2(x_{ai}-x_{bi})} = \cos(\theta_i+\theta_{0,i})\,l_{TB} \\ y_{ti} = & \dfrac{-N_{3i}\pm\sqrt{N_{3i}^2-4N_{2i}N_{4i}}}{2N_{2i}} = \sin(\theta_i+\theta_{0,i})\,l_{TB} \end{cases} \tag{7}$$

where $N_{1i}=x_{ai}^2+y_{ai}^2+z_{ai}^2-(x_{bi}^2+y_{bi}^2)-(l_{AT}^2+l_{TB}^2)$, $N_{2i}=\frac{(y_{ai}-y_{bi})^2}{(x_{ai}-x_{bi})^2}+1$, $N_{3i}=2\left[\frac{(y_{ai}-y_{bi})}{(x_{ai}-x_{bi})}\left(\frac{N_{1i}}{2(x_{ai}-x_{bi})}-x_{bi}\right)+y_{bi}\right]$, $N_{4i}=\left(\frac{N_{1i}}{2(x_{ai}-x_{bi})}-x_{bi}\right)^2+y_{bi}^2-l_{TB}^2$.

$$\theta_i = \arctan\left(\frac{y_{ti}}{x_{ti}}\right)-\theta_{0,i} \tag{8}$$

For each desired end-effector position, if $N_{3i}^2-4N_{2i}N_{4i}\geq 0$, the position can be realized by this 6-RSS parallel robot(Otherwise, it is not an available posture).

2.3. Principals for the proper motion range determination

The initial motion range for each rotary actuator is designed as $(-\pi, \pi]$. But limited by the workspace constraint, singularity constraint and the convergence requirement of kinematic solution, the real motion range for the actuators is narrower than the initial designed one. A proper motion range will be critical for the trajectory planning and collision avoidance work of the 6-RSS parallel robot, and it should satisfy the following requirements.

1. The ability to cover the biggest available workspace: The available workspace of robot is believed to be the union of all its constant-orientation workspaces[6,7], and we can use the boundary of available or reachable workspace to determine the biggest proper motion range.
2. Singularity-free Requirement: For the safety of the 6-RSS parallel robot, it should be singularity-free in the proper motion range of actuators.
3. The uniqueness for the kinematic solution: In some research, the inverse kinematic mapping of the parallel robot is denoted as follows:

$$f : N \to M, \theta = \mathbf{f}(\mathbf{p}); \theta = [\theta_\mathbf{1}, \theta_\mathbf{2}, ..., \theta_\mathbf{6}]^\mathbf{T}, \mathbf{p} = [\mathbf{x}, \mathbf{y}, \mathbf{z}, \gamma, \alpha, \beta]^\mathbf{T} \tag{9}$$

where M is the actuator parameter space(joint space) and N is the Special Euler space for end-effector motion; γ, α and β is the roll angle, pitch angle and yaw angle of the end-effector in *xyzo* frame.

For any point in N, the kinematic mapping f has 64 solutions(imaginary,multiple roots included) based on Eq. (7), and even more periodic solutions exist when solving Eq. (8) in $(-\pi, \pi]$. And if the direct kinematic f^{-1} exist, there may have 40 direct kinematic solutions for a determined θ [27]. To avoid the numerical calculation processing of either inverse or direct kinematic converging to the wrong solution, special motion domain and constraint conditions should be determined.

3. PROPOSED METHODS FOR DETERMING THE PROPER MOTION RANGE

3.1. Minimum motion range from the available workspace

As a union of all constant-orientation workspace $U \subset N$, the available workspace can be determined by similar constraints of constant-orientation workspace introduced in [6, 7]. For any fixed orientation $\mathbf{u} = (\gamma_\mathbf{u}, \alpha_\mathbf{u}, \beta_\mathbf{u})^\mathbf{T}$, it satisfies the following formula.

$$A_{u,i} = R_u A_{0,i} + O' = \begin{bmatrix} M_{u,i}(1) \\ M_{u,i}(2) \\ M_{u,i}(3) \end{bmatrix} + \begin{bmatrix} x \\ y \\ z \end{bmatrix} = \begin{bmatrix} x_{u,ai} \\ y_{u,ai} \\ z_{u,ai} \end{bmatrix} \tag{10}$$

where $M_{u,i}(j), j = 1,2,3$ is a constant value determined by $A_{0,i}$ and rotation matrix R_u. Then, any point $(x,y,z)^T$ belongs to U_u should satisfy the following inequalities.

$$(x - x_i)^2 + (y - y_i)^2 + (z - z_i)^2 \leq l_{AT}^2, (i = 1,2,...,6) \tag{11}$$

where $x_i = x_{bi} - M_{u,i}(1) + \cos(\theta_i + \theta_{0,i})\, l_{TB}$, $y_i = y_{bi} - M_{u,i}(2) + \sin(\theta_i + \theta_{0,i})\, l_{TB}$, $z_i = -M_{u,i}(3)$.

Normally, when the constraint inequalities(like Eq. (10)) determined, point clusters are used to represent the robot constant-orientation workspace. The points inside or on the workspace surfaces are selected by princepels like Monte Carlo method [28] or fixed-interval method[29]. But in a 6-RSS parallel robot, the surface of constant-orientation workspace consists of the end-effector "stationary configurations"[15], which happens to be the "limit position" of one or more RSS chain. Then another method for constant-orientation workspace determination is finding the simple representation of the "stationary configurations", which belongs to the "bifurcation surfaces" to be defined in the next subsection. In this paper, the "stationary configurations" occur when $N_{3i}^2 - 4N_{2i}N_{4i} = 0$, which is a group of 3-D surfaces in world frame *xyzo*. In Figs 3 and 4 the constant-orientation workspaces for two given orientations are shown. The points in both

figures are the workspaces determined by fixed-interval method with the constrants shown in Eq. (11); the surfaces in both figures are the workspace boundaries determined by "stationary configurations".

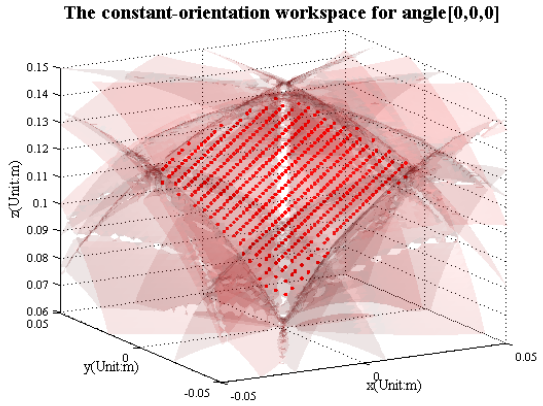

Fig. 3. The constant-orientation workspace-I

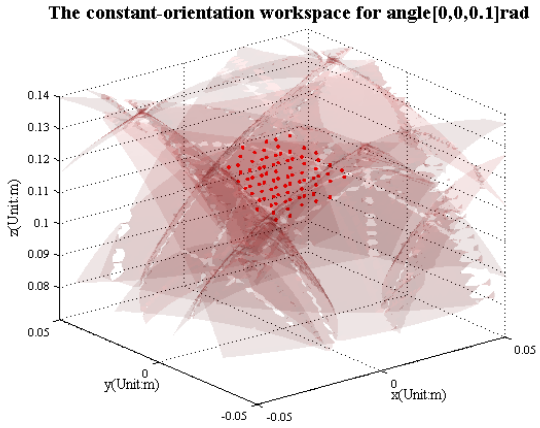

Fig. 4. The constant-orientation workspace-II

3.2. Singularity and Bifurcation constraints for motion range determination

As shown in Fig.2, the velocity projection of A_i and T_i in the bar A_iT_i equals to each other, and we have the following equation:

$$s_i^T \cdot \dot{\theta}_i \cdot l_{T_iB_i} \cdot sw_i = s_i^T \cdot (v_{o'} + \omega_{o'} \times A_i), (i = 1,2,...,6) \tag{12}$$

where $v_{o'}$, $\omega_{o'}$ are the velocity vector and angular velocity vector of the point O', s_i and sw_i are the velocity unit vector for line A_iT_i and T_iO respectively(all values considered in *xyzo* frame).

When cosidering all six chains of the parallel robot, we obtain the velocity kinematic relationship from Eq. (12) as follows[13]:

$$J_1\dot{\theta} = J_2\dot{\mathbf{p}} \tag{13}$$

where $J_1 = diag\left(s_1^T \cdot sw_1 \cdot l_{T_1B_1}, s_2^T \cdot sw_2 \cdot l_{T_2B_2}, \ldots, s_6^T \cdot sw_6 \cdot l_{T_6B_6}\right)$, $J_2 = \begin{bmatrix} s_1^T & \left(A_1 \times s_1^T\right) \\ \vdots & \vdots \\ s_6^T & \left(A_6 \times s_6^T\right) \end{bmatrix}$.

When $\det(J_1) = 0$, it indicates one of (or some of) A_iT_i is perpendicular to the instantaneous velocity of T_i, or A_iT_i happens to project onto the T_iB_i in *xoy* plane. Shown in Fig.5(a-b), with a geometric analysis, a sufficient condition for $\det(J_1) = 0$ is "the ball with a center A_i tangents to the circle with a center B_i in the single point T_i ". The algebraic expression for this sufficient condition can be deduced from (5), then we have the Eq. (14a). From Fig.5c, another sufficient condition for $\det(J_1) = 0$ is shown as Eq. (14b).

$$\prod_{i=1}^{6}\left(N_{3i}^2 - 4N_{2i}N_{4i}\right) = 0 \Rightarrow \det(J_1) = 0 \tag{14a}$$

$$\prod_{i=1}^{6}(|x_{ai} - x_{bi}| + |y_{ai} - y_{bi}|) = 0 \Rightarrow \det(J_1) = 0 \tag{14b}$$

The parallel robot status with $\det(J_1) = 0$ is defined as bifurcation here (the first kind of singularity in [13]). Bifurcation occurs when the force or torque from parallel robot actuators fail to affect the end-effector but the robot still keeps stability. Shown in Fig.6, the sign of each element in the diagonal of J_1 reveals the relative position of the A_iT_i and T_iB_i. Then the sign of these elements can be used to determine whether the chain has crossed a bifurcation. If all the diagonal elements of J_1 keep their signs inside a motion range of actuators, the parallel robot has a uniqueness inverse kinematic solution in this range, as other solutions have been separated by the bifurcation surfaces.

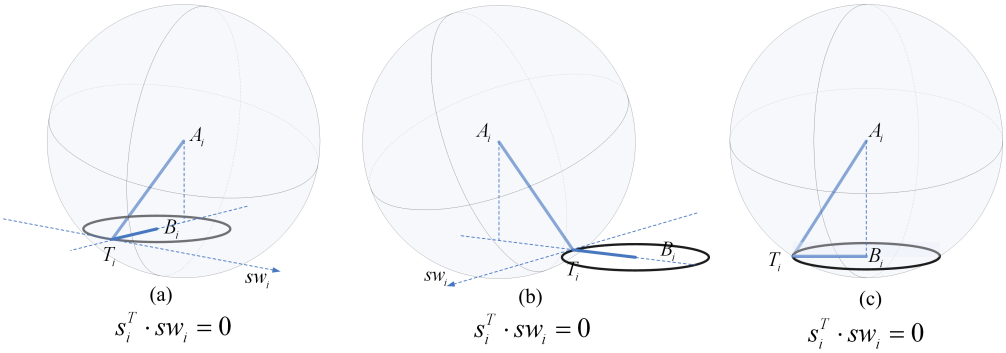

Fig. 5. Geometric relationship and the bifurcation configuration.

Based on line geometry [8], singularity occurs when the orientation vector of the forces and torques acted on the end-effector are coupling to each other. We assume singularity for 6-RSS parallel robot occurs when $\det(J_2) = 0$(The second singularity in [13]). To avoid the perturbation from degenerate singularity surface, the Cauchy Index of J_2 can be used to determine the singularity based on the conclusion of [25]. Then for any two very closing points $p_1, p_2 \in M$, the singularity constraint condition is given as follows:

1) $\left|\Delta_{p_1}^{J_2} - \Delta_{p_2}^{J_2}\right| = 0$, line p_1p_2 still in a simple connected singularity-free domain;
2) $\left|\Delta_{p_1}^{J_2} - \Delta_{p_2}^{J_2}\right| = 2$, line p_1p_2 cross a non-degenerate singularity surface;
3) $\left|\Delta_{p_1}^{J_2} - \Delta_{p_2}^{J_2}\right| > 2$, and in line p_1p_2,$\min\det(J_2) = 0$, line p_1p_2 cross a degenerate singularity surface.

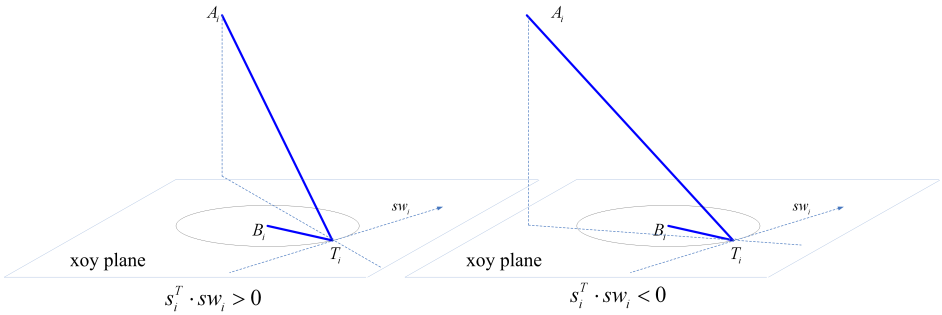

Fig. 6. Elements sign and the relative position.

3.3. Uniqueness of kinematic solution and Robust direct kinematic algorithm

As introduced in last subsection, the bifurcation surfaces may separate the inverse kinematic solutions of the 6-RSS parallel robot used in this research. Then the bifurcation-free constraint is a sufficient condition for the uniqueness of inverse kinematic.

The uniqueness problem for direct kinematic calculation is more complex, which can be transformed into a bijective relationship proof. In this research, we proposed a robust direct kinematic algorithm to determine the uniqueness of direct kinematic solution by numerical verification.

Normally, the numerical direct kinematic methods like Newton-Raphson method[16], Jacobi method[30] and Powell method[31] can achieve high accuracy in the parallel robot analysis with small workspace(which means the initial pose is not far from the final result). But all these normal direct kinematic methods may fail to refresh the value of $\mathbf{p}$ when either $\det(J_1) = 0$ or $\det(J_2) = 0$. Then the iteration can be trapped by a local minimum solution. Even the methods without using Jacobian matrix(like Powell method and DSC method) may be affected by the bifurcation or singularities.

Here we present a quasi-Gough method to obtain the direct kinematic solution of the 6-RSS parallel robot. For our 6-RSS parallel robot, once the actuators output θ is known, the whole kinematic information of T_i is determined. As the T_i can be redefined as the base terminals of a Gough platform, we can deform the 6-RSS parallel robot into a quasi-gough mechanism. Then we need to solve the direct kinematic problem of a Gough-platform with actuators' length equal to $\mathbf{l}_{AT} = (l_{A_1T_1}, \ldots, l_{A_6T_6})^T$, end-effector terminals A_i and base terminals T_i. And fortunately, there is no disturbance from singularity for the direct kinematic of this new "gough-platform".

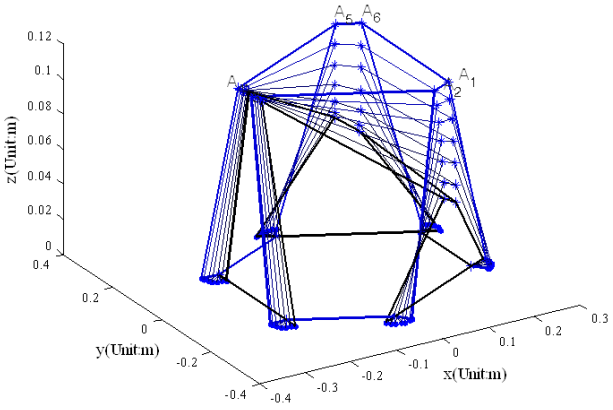

Fig. 7. Procedure of normal direct kinematic method

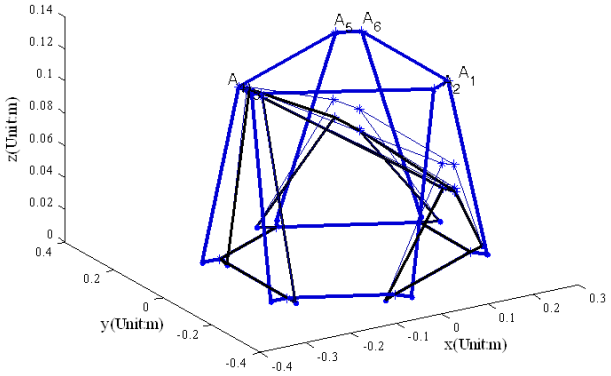

Fig. 8. Procedure of quasi-Gough method

The normal direct kinematic methods mentioned above search the solutions from the actuator workspace directly, which means all the temporary status appearing during the iteration can be realized by the real 6-RSS parallel robot. Different from the normal methods, the quasi-gough method use a increase Δl but not $\Delta\theta$ in the iteration procedurce, and only the calculation result can be really achieved by the real mechanism. If $\| \ \|_*$ denotes the norms in corresponding parameter space, the quasi-Gough direct kinematic algorithm is given as follows:

1) Input the desire actuators angles θ, and calculate the corresponding $T_i (i = 1,2,...,6)$ for the quasi-Gough platform, choose the initial position of $\mathbf{p}$ based on initial status of the end-effector. Set the condition coefficient ε_c for the iterated result accuracy, set the penalty coefficient ε_p for position correction;
2) Calculate a position correction $\Delta\mathbf{p}$ through any above-mentioned nonlinear direct kinematic algorithms based on $\Delta\mathbf{l} = \mathbf{l}_{AT} - f(\mathbf{p})$;
3) If $\|f(\mathbf{p}, \Delta\mathbf{p})\|_* \leq \varepsilon_p$, then $\mathbf{p} = \mathbf{p} + \Delta\mathbf{p}$; else, back to step 2) for a new $\Delta\mathbf{p}$;
4) If $\|f(\mathbf{p}, \mathbf{l}_{AT})\|_* \leq \varepsilon_c$, then output the present $\mathbf{p}$ as the result; else, back to step 2) for a new iteration.

Figs 7 and 8 show the procedures of the two direct kinematic methods (normal method and quasi-Gough method). The blue sketches are the initial status of the 6-RSS parallel robot, and the black sketches are the final status for the direct kinematic solutions. In Fig.7, the numerical iteration steps are limited by penalty coefficient, and there exists a maximun step limit for the modification of θ. In Fig.8, the solution is determined in less steps than the previous one, and the length of A_iT_i convergence into $l_{A_iT_i}$ fastly. The quasi-Gough method is applied in the simulation, and the direct kinematic are solved for all input actuator angles.

4. SIMULATION AND RESULTS

Figs 9 and 10 show the 6-RSS parallel robot we used in this research.

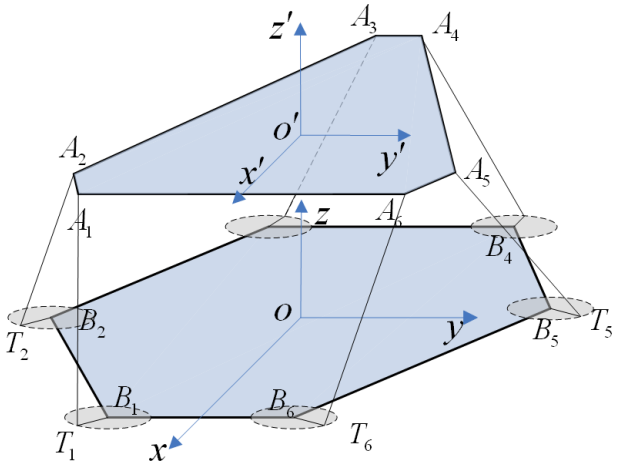

Fig. 9. The 6-RSS parallel robot coordinate definition

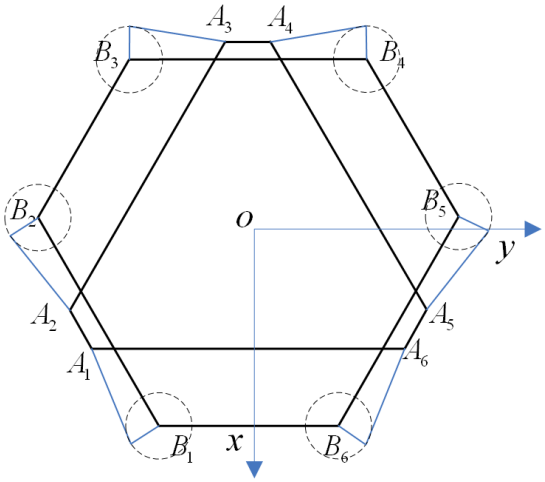

Fig. 10. A vertical view of the 6-RSS parallel robot

The rotary vector for the 6-RSS parallel robot is $w_{1-6} = [0,0,1]^T$, both the fix base and end-effector are hexagons. And based on the mechanism structure parameters, the terminal coordinates in corresponding coordinate system are presented in Table.1. Assume the kinematic calibration is done.

Table 1. Terminal coordinates for the 6-RSS parallel robot

	A'_i coordinates in $x'y'z'o'$ frame/mm	B_i coordinates in $xyzo$ frame/mm
Chain 1	$A'_1(131.3,-177.5,0)$	$B_1(221.4,104.5,0)$
Chain 2	$A'_2(88,-202.5,0)$	$B_2(20.2,-224,0)$
Chain 3	$A'_3(-219.4,-25,0)$	$B_3(-201.2,-139.5,0)$
Chain 4	$A'_4(-219.4,25,0)$	$B_4(-201.2,139.5,0)$
Chain 5	$A'_5(88,202.5,0)$	$B_5(-20.2,-224,0)$
Chain 6	$A'_6(131.3,177.5,0)$	$B_6(221.4,104.5,0)$

4.1. Determination for minimum reachable actuator motion range

As shown in Eq. (9), if we set the initial actuator angles $\theta_{0,i}$ to be the zero points, the available workspace should be realized by a minimum actuator motion range $(-0.5\pi, 0.5\pi]$. The available workspace is the sum of constant-orientation workspaces, and its projection in Cartesian space is defined as reachable workspace U_R. To determine the minimum motion range for reachable workspace, we apply a posture searching method here and select the searching trajectories from the surface of U_R(shown in Fig.11). It is noted that the selection of $\theta_{0,i}$ affects the searching results directly(shown in Fig.12). The objective of in this subsection is to find the optimal initial actuator angles for the minimum reachable actuator motion range $(-0.5\pi, 0.5\pi]$. The optimal objective function for initial actuator angles is defined as follows:

$$\min_{U} \sum_{i=1}^{6} \left(\left| \theta'_{max,i} - \theta'_{min,i} \right| + \lambda \left| \theta'_{max,i} + \theta'_{min,i} - 2\theta_{0,i} \right| \right). \tag{15}$$

Because the rotations of these six chains are totally decoupled, the objective function for each chain can be rewritten as follows:

$$\min_{U_R} \left(\left| \theta'_{max,i} - \theta'_{min,i} \right| + \lambda \left| \theta'_{max,i} + \theta'_{min,i} - 2\theta_{0,i} \right| \right). \tag{16}$$

Notice that the period of the circle angle should be considered as well. The searching algorithm is summarized in the following steps:

1) Determine the available workspace U under Eq. (11), and obtain the reachable workspace U_R ;
2) Choose the terminal points in the surface of U_R, and generate the searching trajectories from them;
3) Traverse in the range of $(-\pi,\pi]$ with the step value $\Delta\theta_{0,i}$ and choose the initial angle for each limb;
4) In each step, obtain the inverse kinematic solution close to the initial angle by Eqs. (8) and (9);
5) Find the initial angle for each limb with the constraint of Eq. (16).

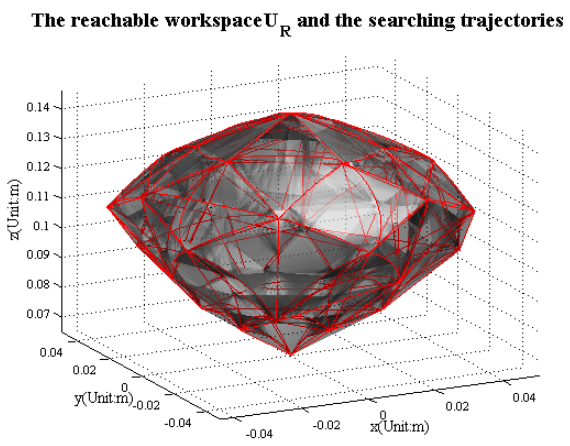

Fig. 11. Reachable workspace and searching trajectories

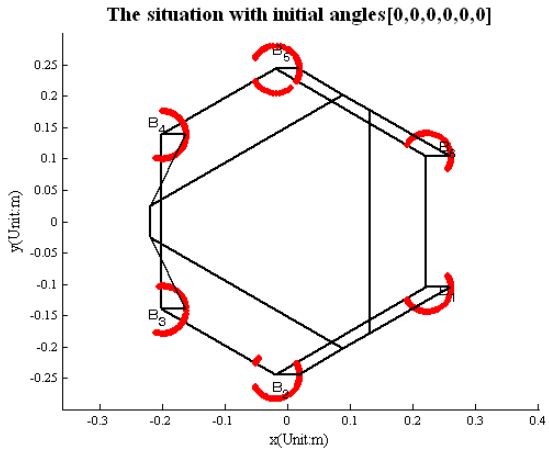

Fig. 12. Solution range for initial angle(0,0,0,0,0,0)

If $\lambda = 0.5$, the objective functions reach their minimums in the value $[-\pi/3,-\pi/3,\pi,\pi,\pi/3,\pi/3,]$ (shown in the Fig.13). And the minimun reachable motion range for actuators can be easily determined when the optimal $\theta_{0,i}$ is chosen(shown in Fig.14).

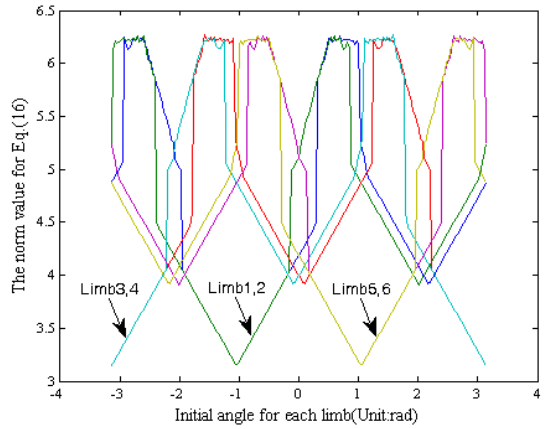

Fig. 13. The optimization for reachable motion range

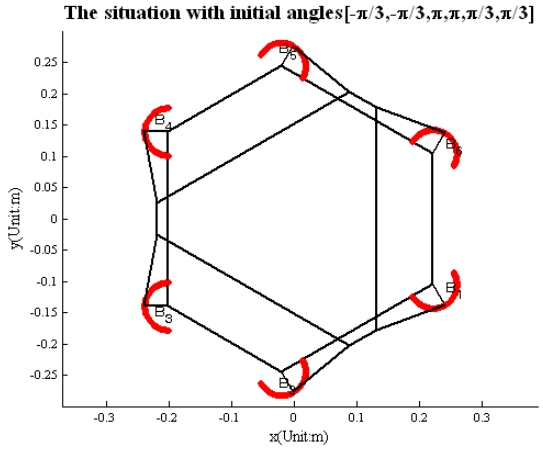

Fig. 14. The optimal initial angles and motion range

4.2. Determination for singularity-free and bifurcation-free actuator motion range

After verification, the reachable rotary motion range obtained in last subsection is not bifurcation-free, and more work should be done to determine a proper actuators motion range. Shown in Eq. (9), the output angles of the actuators are based on the reference of initial angles, and the objective function for the 6-RSS parallel robot under singularity-free and bifurcation-free constraints is given as follow[25]:

$$\max_{(-\pi/2,\pi/2]} \sum_{i=1}^{6} \lambda_i \left|\theta_{max,i} - \theta_{min,i}\right| \tag{17}$$

Eq. (17) can be simplified based on the symmetric structure of the 6-RSS-parallel. Then the optimization problem can be transformed into a single-objective planning: finding the maximum of Eq. (17) under singularity-free and bifurcation-free constraint conditions when $\theta_{max} = \theta_{max,i}, \theta_{min} = \theta_{min,i}, (i = 1,2,...,6)$.

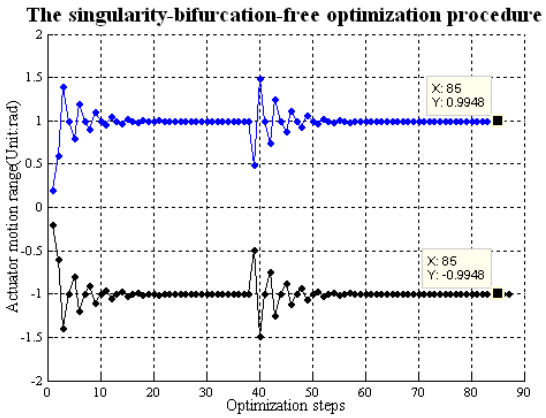

Fig. 15. The singularity & bifurcation-free optimization

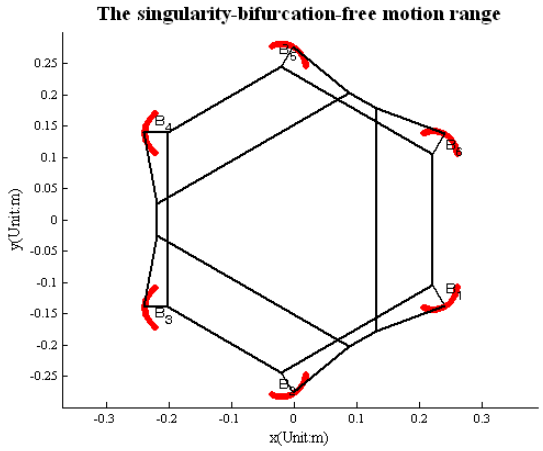

Fig. 16. Optimal initial angles with proper motion range

The optimization is similar to the method proposed in [25]. And the constraint conditions we used here are listed as follows:

1. Bifurcation-free condition $sign(J_1) = [+,-,+,-,+,-]$;
2. Singularity-free condition $\Delta^{J_2} = 0$ and $\det(J_2) \neq 0$.

The optimization procedure is shown in Figs.15 and16, and the maximum motion range in which the 6-RSS parallel robot is singularity-free and bifurcation-free is $(-0.9948rad, 0.9948rad)$.

5. CONCLUSION

In this paper, a thorough kinematic analysis of general 6-RSS parallel robot has been conducted. The novel methods for available workspace determination, singularity analysis and bifurcation avoidance for 6-RSS parallel robot are proposed respectively. The simulation results validate the effectiveness of the proposed methods. And the proper actuator motion range, in which the robot owns the biggest, singularity-free and bifurcation-free workspace is determined for a special 6-RSS parallel robot. In the future work, the proposed method will be applied in the kinematic analysis of other types of 6-RSS parallel robots.

REFERENCES

1. Merlet, J.P. *Parallel robots*, Vol. 74. Springer Science & Business Media, 2001.
2. Tsai, L.W. "Systematic enumeration of parallel manipulators." In "Parallel Kinematic Machines," pp. 33–49. Springer, 1999.
3. McCarthy, J.M. *Geometric design of linkages*, Vol. 11. Springer Science & Business Media, 2000.
4. Hunt, K. "Structural kinematics of in-parallel-actuated robot-arms." *Journal of Mechanical Design*, Vol. 105, No. 4, pp. 705–712, 1983.
5. Dasgupta, B. and Mruthyunjaya, T. "The stewart platform manipulator: a review." *Mechanism and machine theory*, Vol. 35, No. 1, pp. 15–40, 2000.
6. Bonev, I. and Gosselin, C.M. "A geometric algorithm for the computation of the constant-orientation workspace of 6-rus parallel manipulators." In "Proc. of the 2000 ASME Design Engineering Technical Conferences," Montreal, Canada, 2000.

7. Bonev, I. and Ryu, J. "A new approach to orientation workspace analysis of 6-dof parallel manipulators." *Mechanism and Machine Theory*, Vol. 36, No. 1, pp. 15–28, 2001.
8. Merlet, J.P. "Singular configurations of parallel manipulators and grassmann geometry." *The International Journal of Robotics Research*, Vol. 8, No. 5, pp. 45–56, 1989.
9. Hunt, K.H. *Kinematic geometry of mechanisms*. Clarendon Press Oxford, 1990.
10. Park, F. and Kim, J.W. "Singularity analysis of closed kinematic chains." *Journal of mechanical design*, Vol. 121, No. 1, pp. 32–38, 1999.
11. Ghosal, A. and Ravani, B. "A differential-geometric analysis of singularities of point trajectories of serial and parallel manipulators." *Journal of Mechanical Design*, Vol. 123, No. 1, pp. 80–89, 2001.
12. Liu, X.J., Wang, J., Gao, F. and Wang, L.P. "Mechanism design of a simplified 6-dof 6-rus parallel manipulator." *Robotica*, Vol. 20, No. 01, pp. 81–91, 2002.
13. Gosselin, C.M.and Angeles, J. "Singularity analysis of closed-loop kinematic chains." *Robotics and Automation, IEEE Transactions on*, Vol. 6, No. 3, pp. 281–290, 1990.
14. Pierrot, F., Dauchez, P. and Fournier, A. "Hexa: a fast six-dof fully-parallel robot." In "Proc. of 1991 Fifth International Conference on Advanced Robotics," pp. 1158–1163. IEEE, 1991.
15. Zabalza, I., Ros, J., Gil, J., Pintor, J. and Jiménez, J. "A variant of a 6-rks hunt-type parallel manipulator to easily use insensitivity position configurations." In "Advances in Robot Kinematics," pp. 291–300. Springer, 2002.
16. Parrish, R., Dieudonné, E. and Bardusch, R. "An actuator extension transormation for a motion simulator and an inverse transformation applying newton-raphson's method." *NASA Technical report D-7067*, 1972.
17. Mu, Z.L. and Kazerounian, K. "A real parameter continuation method for complete solution of forward position analysis of the general stewart." *Journal of Mechanical Design*, Vol. 124, No. 2, pp. 236–244, 2002.
18. Ramesh Kumar, P. and Bandyopadhyay, B. "The forward kinematic modeling of a stewart platform using nlarx model with wavelet network." In "Proc. of 2013 11th IEEE International Conference on Industrial Informatics,," pp. 343–348. IEEE, Bochum, Germany, 2013.
19. Dehghani, M., Safavi, A., Khayatian, A., Ahmadi, M. and Eghtesad, M. *Neural network solutions for forward kinematics problem of HEXA parallel robot*. INTECH Open Access Publisher, 2008.
20. Huang, X.G., Wei, S.M., Qiang, X. and Huang, S.G. "Forward kinematics of the 6-6 stewart platform with planar base and platform using algebraic elimination." In "Proc. of 2007 IEEE International Conference on Automation and Logistics," pp. 2655–2659. IEEE, Jinan, China, 2007.
21. Jiang, Q.M. and Gosselin, C.M. "Determination of the maximal singularity-free orientation workspace for the gough–stewart platform." *Mechanism and Machine Theory*, Vol. 44, No. 6, pp. 1281–1293, 2009.
22. Li, H., Zhang, Y. and Yang, Y. "Singularity-free taskspace optimization of 6-rss mechanisms." In "Proc. of ASME 2009 International Design Engineering Technical Conferences and Computers and Information in Engineering Conference," pp. 1237–1244. American Society of Mechanical Engineers, 2009.
23. Martinez, E.E.H., Peña, S.I.V. and Soto, E.S. "Towards a robust solution of the non-linear kinematics for the general stewart platform with estimation of distribution algorithms." *Int J Adv Robotic Sy*, Vol. 10, No. 38, 2013.
24. Coste, M. "Asymptotic singularities of planar parallel 3-rpr manipulators." In "Latest Advances in Robot Kinematics," pp. 35–42. Springer, 2012.
25. Zeng, R., Zhao, Y.J. and Dai, S.L. "The proper motion domain for the actuators of stewart-gough platform." In "Proc. of 2014 IEEE Chinese Guidance, Navigation and Control Conference," pp. 1706–1711. IEEE, 2014.
26. Zhang, X.M., Xie, W.F. and Hoa, S.V. "Modeling and workspace analysis of collaborative advanced fiber placement machine." In "Proc. of ASME 2014 International Mechanical Engineering Congress and Exposition," Montreal, Canada, 2014.
27. Raghavan, M. "The stewart platform of general geometry has 40 configurations." *Journal of Mechanical Design*, Vol. 115, No. 2, pp. 277–282, 1993.
28. Alciatore, D. and Ng, C. "Determining manipulator workspace boundaries using the monte carlo method and least squares segmentation." *ASME Robotics: Kinematics, Dynamics and Controls*, Vol. 72, pp. 141–146, 1994.
29. Bohigas, O., Manubens, M. and Ros, L. "A linear relaxation method for computing workspace slices of the stewart platform." *Journal of Mechanisms and Robotics*, Vol. 5, No. 1, p. 011005, 2013.
30. Wilkinson, J.H., Wilkinson, J.H. and Wilkinson, J.H. *The algebraic eigenvalue problem*, Vol. 87. Clarendon Press Oxford, 1965.
31. Powell, M.J. "A hybrid method for nonlinear equations." *Numerical methods for nonlinear algebraic equations*, Vol. 7, pp. 87–114, 1970.